JOURNAL OF MATERIALS SCIENCE 30 (1995) 5755–5762

Response dynamics of the lamellar spacing for Al–Si eutectic during directional solidification

J. M. LIU, Z. C. WU, Z. G. LIU
National Laboratory of Solid State Microstructures, Nanjing University, Nanjing 210093, People's Republic of China

The response of the lamellar spacing to abrupt change of the solidifying rate for Al–Si eutectic during directional solidification has been investigated both experimentally and theoretically. When the solidifying rate was changed abruptly, the response of the lamellar spacing was gradual and retarded, which was attributed to the "cluster branching" and "cluster terminating" mechanisms of the lamellar phases. The retarded distance, as a function of the abrupt change factor, ρ, for both $\rho > 1$ and $\rho < 1$, has been evaluated, and the uniqueness of the spacing selection has been verified. A theoretical approach of the response dynamics has been presented by considering the solute diffusion in liquid and the growth anisotropy effect of the eutectic lamella. A dynamic factor has been introduced to characterize the growth anisotropy. Excellent agreement between the theoretical approach and the measured results has been shown. Finally, this theory has been successfully applied to describe non-steady-state directional solidification of Al–Si eutectic with constant accelerating solidification rate.

1. Introduction

The problem of spacing selection of lamellar eutectics during directional solidification (DS) has received interest both from the viewpoint of technological applications during the last few decades [1–4], and also as a representative example of spontaneous pattern formations which have been attracting theorists in recent years [5–10]. For the case of steady-state solidification, the solidifying interface forms parallel lamellae of two coexisting solid phases: α and β. The central problem is the mechanism dominating selection of the lamellar spacing, λ. For this topic, many theories have been developed [11–16], including the recently developed similarity laws [17–21]. The dynamic fluctuations during DS with constant solidifying rate, V, and temperature gradient, G_L, which result in the generation and transfer of a tilting wave along the solidifying interface, have been investigated in detail [17–21].

However, as an event occurring in practice, the non-steady state solidification of lamellar eutectic is not understood well. An approach to this problem suggests the two fundamental problems for DS of lamellar eutectics: (1) spacing selection dynamics for fixed V and G_L: (2) the response of the spacing to fluctuations during DS, including transfer of the tilting waves on the solidifying interface. To our knowledge, this problem has only been studied in a few cases [22–26]. As V or G_L change, the solute field in the liquid will respond and then an adjustment of the spacing, λ, will follow. Mollard and Flemings [22, 23] calculated the response of solute diffusion in a liquid to an abrupt change of V. They claimed that the diffusion was so rapid that the response would end within the length $L = D_L/V$, where D_L represents the diffusion coefficient of the solute in the liquid. Carlberg and Fredriksson [24] investigated the spacing response to an abrupt change of V for DS of Al–Al_2Cu eutectic. They showed that the response was abrupt but slightly retarded, although the dependence of the retarded distance on the abrupt change of V was not presented. The sudden splitting (or terminating) of the lamellae was observed as a dynamic mechanism responsible for the response of the spacing. In addition, the evolution of the eutectic structure modified by a sodium-based modifier during DS of Al–Si eutectic with constant accelerating solidification rate has been studied [25].

It should be pointed out that in all these studies the response dynamics of λ to variation of V or G was ignored. It is still not clear what is involved in the transition dynamics from an initial state to a final one, after fluctuations of V or G_L occurred. Is the final state unique or path-correlated? Does the adjustment of λ only depend on the response of solute diffusion in a liquid? Besides the sudden splitting (or terminating) mechanism, does another structure response mechanism exist to fluctuations of V and G_L. The answers to these problems will be of interest for a deep insight into the spacing selection dynamics for lamellar eutectics during directional solidification.

In the present work, the non-steady-state directional solidification of Al–Si eutectic was studied. The reasons for selecting this system were that it is interesting from the viewpoint of application, and a new structure response mechanism was previously

0022–2461

observed. Particular attention was paid to the response dynamics of λ to fluctuations of solidification rate, V. For a generality consideration, the fluctuations are assumed to be an abrupt change of V from an initial rate, V_1, to an end rate, V_2, because any fluctuation of V during non-steady-state solidification can be approached by a series of abruptly changing steps with $V_2 = V_1 + dV$, where dV is the derivative of V. The transition of the lamellar structure from an initial spacing to an end spacing, and the structure response mechanism responsible for the transition, after the abrupt change of V, were investigated in detail. It is shown that the response is gradual and seriously retarded. A new mechanism for the spacing response was observed. Based on the experimental observations, a theoretical approach of the response dynamics is presented, which shows an excellent agreement with the experiments.

2. Experimental procedure

The experiments were performed on a unidirectional solidification apparatus. For detail of the DS experiments, see our previous reports [27, 28]. The samples with a nominal composition of Al–12.62 at % Si were prepared by melting high-purity aluminium and single crystals of silicon in a vacuum induction furnace and casting into cylindrical bars of diameter 8 mm × 140 mm. Each sample was set into a high-purity graphite tube, which was placed vertically into an alumina pipe surrounded by two heaters. The sample was first heated to 1000 °C and then held for 30 min. The graphite tube was then lowered into a freezer connected to the bottom of the alumina pipe. The cooling medium in the freezer was liquid Ga–In–Sn alloy with a freezing point of 5 °C. The freezer and the alumina moved upwards relative to the sample at a speed V_P. Because the freezer could effectively cool the end part of the sample, the temperature distribution in the liquid zone ahead of the solid–liquid interface remained linear and unchanged and so G_L was then constant during DS. In the experiments, the end part of each sample which had been melted was first immersed into the liquid alloy contained by the freezer for 10 mm and held for 10 min to guarantee formation of an equilibrium solid–liquid interface. After the experiment, the position of this interface could be observed by etching the sample in HF agent, and this was then selected as the starting point of the response curve measurements. Because λ was ~ 10 μm, a steady state was considered to be reached after an initial solidification of 10 mm. Each sample grew for 8–10 cm, during which one or more abrupt changes of V were performed; the sample was then quenched into water at room temperature.

Our measurements showed that effective cooling of the freezer can guarantee synchronization of the moving speed, V_P, of the freezer and the solidification rate, V, of the sample, provided $V \leq 120\ \mu m\ s^{-1}$. An experiment for checking this synchronization was performed by accelerating the freezer from $V_P = 0$ to $V_P = 120\ \mu m\ s^{-1}$ with an acceleration, a, and then quenching the sample into water. As $a \leq 2.0\ \mu m^2\ s^{-1}$, the distance between the initial solid–liquid interface and the quenched solidifying interface $S_a \cong \frac{1}{2}at^2$, where t is the solidification time. This clearly showed that V indeed synchronized with V_P, otherwise we should have $S_a \ll \frac{1}{2}at^2$. Therefore, V was taken to be equal to V_P.

In the present work, a special controlling unit was designed to change V of the sample from an initial value of V_1 to a final value of V_2 within 1 s for realizing the abrupt change of V. This interval had virtually no influence on the response curve because the transition distance between the two steady states at $V = V_1$ and $V = V_2$ was of the order of millimetres. After the abrupt change, the sample was held to solidify at the rate V_2 for a distance which was much larger than the transition distance between the two steady states. An abrupt change factor, ρ, was defined as

$$\rho = V_2/V_1 \quad (1)$$

to represent the magnitude of the abrupt change of V. The response curve was presented by plotting the spacing, λ, of the lamellar structure against the solidifying distance, S. A schematic drawing of the response curve is given in Fig. 1, where the sample solidified at a rate V_1 for some distance; the abrupt change of V from V_1 to V_2 occurred at the vertical dashed line position, and then the sample solidified at V_2 until the end. The horizontal solid line in zone $V = V_1$ represents the spacing, denoted by λ_{S1}, as the sample solidified at a rate V_1 in a steady state; the horizontal solid line in zone $V = V_2$ represents the spacing, denoted by λ_{S2}, as the sample solidified at a rate V_2 in a steady state. The wavy curve, labelled by λ, is the measured response curve. As V changed from V_1 to V_2, λ would shift from λ_{S1} to λ_{S2} and the transient distance, defined as the retarded distance, is denoted by S_r, as indicated in Fig. 1. In this work, S_r, as a critical parameter characterizing the response dynamics, has been evaluated experimentally and theoretically.

The solidified samples were cut longitudinally. The lamellar spacing, λ, was measured on the longitudinal sections using a micrometer in a microscope. The equilibrium solid–liquid interface before solidifying was selected as the starting point for spacing measurements. Apart from this initial position, the

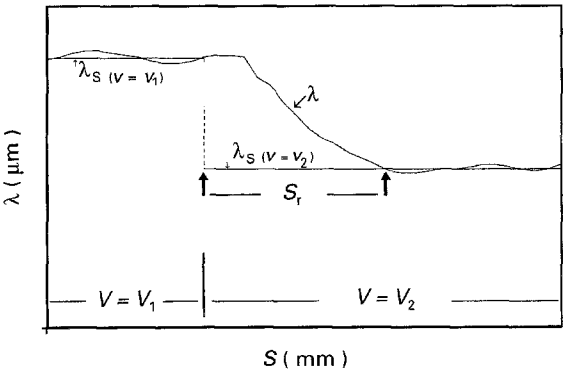

Figure 1 A schematic drawing of the response curve of the spacing, λ, to one abrupt change of V from V_1 to V_2.

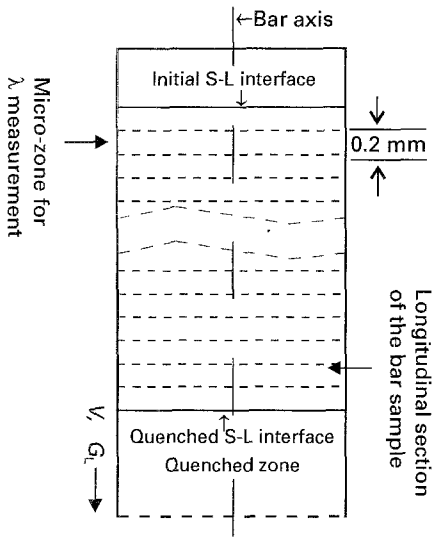

Figure 2 A schematic drawing of division of the micro-zones on the longitudinal section of a bar-like sample for measurement of the spacing, λ, as a function of the solidifying distance, S. Each micro-zone has a width of 0.2 mm along the axis of the sample.

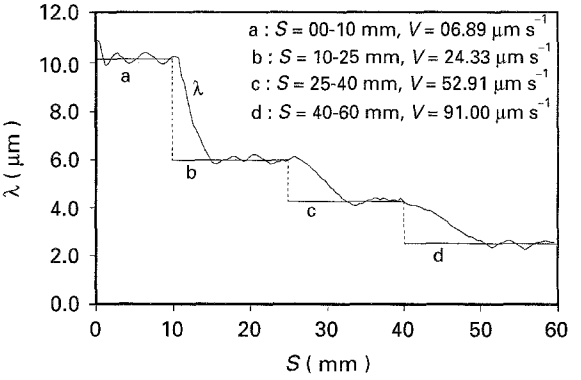

Figure 3 The measured response curves of the spacing, λ, to three abrupt change of V for the case of $\rho > 1$. The solidification rates for the four ranges are shown.

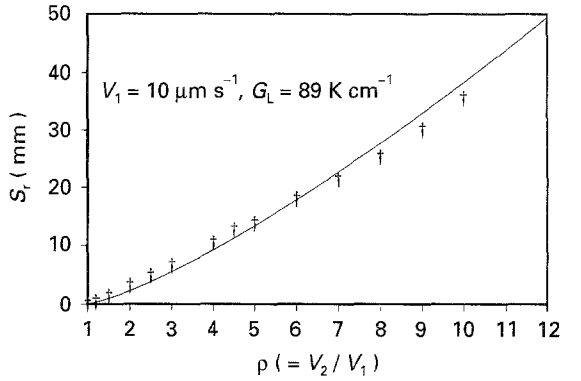

Figure 4 The (†) measured and (——) calculated retarded distance, S_r, as a function of the abrupt change factor, ρ, at a fixed V_1 for the case of $\rho > 1$.

longitudinal section for each sample was divided into micro-zones of 0.2 mm long along the axis of the cylindrical bar. The micro-zone division is schematically drawn in Fig. 2. Owing to the irregularity of the solidified structure of the Al–Si eutectic, in each micro-zone 20 lamellar spacings were measured at different fields of view and the average value of the data was treated as the measured λ. For detail of the spacing measurement in each micro-zone, see our previous report [27], where the measured spacing, λ_S, as a function of V for Al–Si eutectic solidifying in steady-state conditions was also summarized.

3. Results

3.1. Spacing response for $\rho > 1$

For $\rho > 1$, the solidifying interface originally propagating at a lower rate, V_1, was suddenly accelerated to a higher rate, V_2. Experiments for different V_1 and ρ were performed. Fig. 3 gives a representative example, which shows the response curves of three times of abrupt change of V performed on the same sample. It is clearly shown that for each abrupt change, the response of λ was not abrupt but gradual and seriously retarded. The retarded distance, S_r, as defined in Fig. 1, represents the distance from the position where the abrupt change of V occurred to the position where the spacing λ reached λ_{S2} from λ_{S1}. It is astonishing that S_r was much larger than the diffusion length, L ($L \cong 10$–100 μm here) and was of millimetres in order of magnitude. Obviously, this fact could not be explained by the numerical approach developed by Mollard and Flemings [22, 23]. We have sufficient reasons to argue that in addition to the solute diffusion in the liquid, there existed a new dynamic mechanism playing a strong role in the response dynamics of λ, which will be discussed below.

The measurements also revealed that for $\rho > 1$, S_r varied as a linearly increasing function of V_1 as $\rho = \text{const}$. As $V_1 = 10\ \mu\text{m s}^{-1}$, the measured S_r as a function of ρ is shown in Fig. 4, where the solid curve is S_r calculated from the theoretical approach to be presented below. As $\rho = 10$, S_r was over 30 mm, showing that transition of λ from λ_{S1} to λ_{S2} was very slow.

Although the response of λ was seriously retarded, after each abrupt change of V the spacing, λ, always shifted towards λ_{S2}. Owing to the irregularity of the Al–Si eutectic structure, the measured spacing showed small fluctuations around λ_{S2}. This indicates that the spacing, λ, of Al–Si eutectic always selected the same value if V and G_L were fixed. The present experiments provide direct evidence for the argument of the uniqueness of spacing selection of lamellar eutectics.

3.2. Spacing response for $\rho < 1$

As $\rho < 1$, the solidifying interface originally propagating at a higher rate, V_1, was decelerated suddenly to a lower rate, V_2. Two examples of the response curves as $\rho < 1$ are shown in Fig. 5a and b. The response features are roughly similar to the cases of $\rho > 1$. However, the retarded distance as $\rho < 1$ seemed to be much larger than that of $\rho > 1$, showing an asymmetrical feature of the response dynamics.

The retarded distance as function of V_1 and ρ were evaluated. When ρ was fixed, S_r showed a linear increase with V_1. When V_1 was held unchanged, S_r as a function of ρ displayed some complex features. The measured results are shown in Fig. 6, where the solid

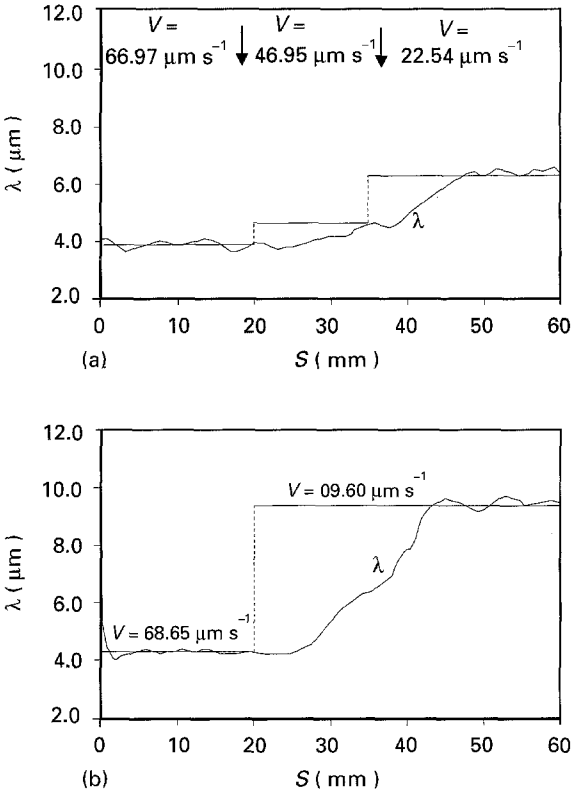

Figure 5 (a, b) The measured response curves of the spacing, λ, to several abrupt changes of V for the case of $\rho < 1$. The solidification rates for the different ranges are shown.

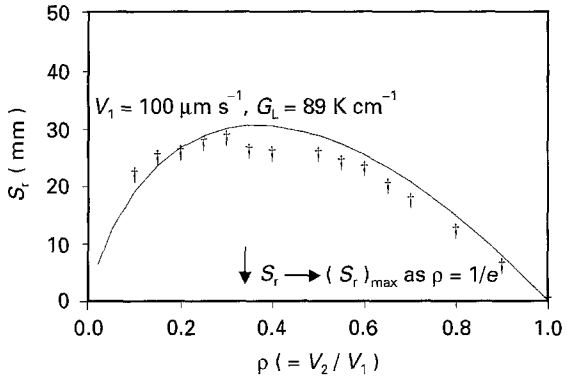

Figure 6 The (†) measured and (——) calculated retarded distance, S_r, as a function of the abrupt change factor, ρ, at a fixed V_1 for the case of $\rho < 1$.

curve is the retarded distance calculated from the theory presented below. Interestingly, the curve of the dependence of S_r on ρ is convex upward and reached the maximum value as $\rho = 0.3$–0.4.

For $\rho < 1$, after each abrupt change of V, the spacing, λ, increased slowly and finally reached λ_{S2}. We can conclude that for samples solidifying at the same steady-state conditions the lamellar spacing should be the same, although the transition towards the final steady state showed a difference for different cases.

3.3. Structure response

As revealed above, the response of λ to an abrupt change of V was gradual. This gradual transition obviously does not support the so-called "sudden splitting" for $\rho > 1$ and "lamella terminating" for $\rho < 1$ [24]. For Al–Si eutectic, the structure irregularity was partially attributed to the fact that silicon lamellae are very easily split and branched. Our observations revealed that the gradual response of λ was due to a new structure response mechanism, termed "cluster-branching" and "cluster-terminating". Only if $\rho > 70$ for the case of $\rho > 1$, the spacing responded by the "sudden splitting" mechanism, followed by the second-order branching of silicon lamellae.

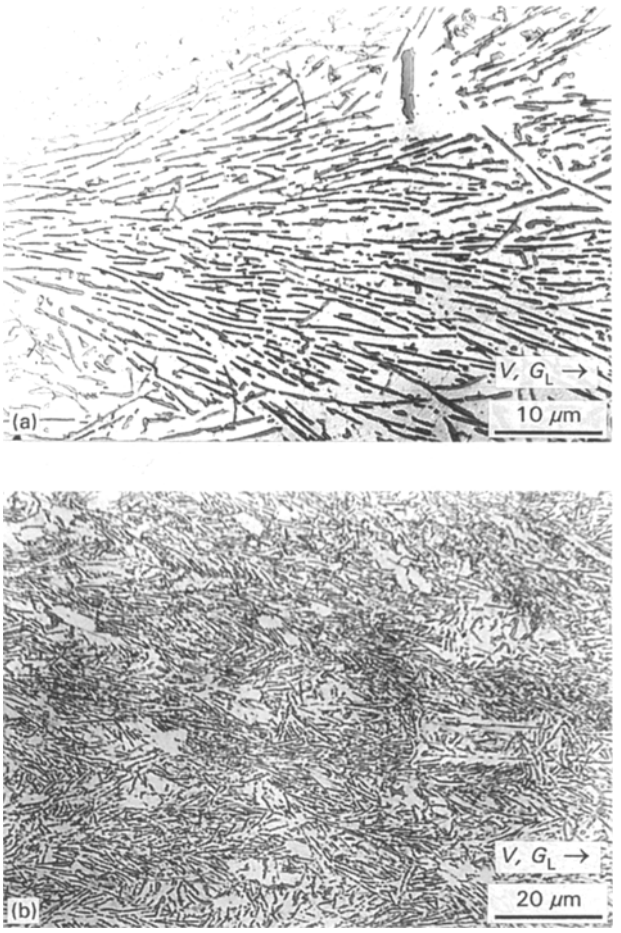

Figure 7 Optical micrographs showing microstructures of Al–Si eutectic within the transition zones. (a) A branching cluster, $V_1 = 47\ \mu m\ s^{-1}$ and $\rho = 1.47$; (b) termination of branching clusters and creation of new clusters, $V_1 = 67\ \mu m\ s^{-1}$ and $\rho = 0.67$.

For $\rho > 1$, an optical micrograph of the branching-cluster is presented in Fig. 7a. In the macroscopic frame, due to this mechanism, the response of λ must be continuous and could be approached as a smoothing and continuum function of time. However, for the "sudden splitting" mechanism, the response must be step-type.

For $\rho < 1$, the structural mechanism for the spacing response was the so-called "branching-cluster terminating", accompanied by the "cluster-branching". An optical micrograph showing the structures in the transition zone is presented in Fig. 7b, which shows that the branching-clusters are small in size and many of them terminated before further extending. Because there were still many branching clusters formed during the transition, the coarsening of the lamellar structure with time was seriously delayed. Therefore, the retarded distance for $\rho < 1$ became much larger than

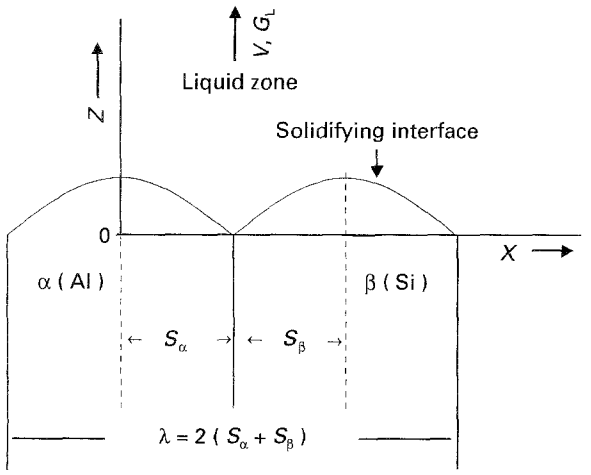

Figure 8 A schematic drawing of the solidifying interface of lamellar eutectic during directional solidification and the coordinates for analysis.

that for $\rho > 1$. These response features can be explained very well by the following theoretical approach through introducing a dynamic factor to characterize the growth anisotropy of the eutectic phases.

4. Theoretical approach

For DS of a lamellar eutectic, it is believed that the spacing of a lamellar structure is determined by the coupling between the solute diffusion in the liquid and the Gibbs–Thomson effect of the solidifying interface. Fig. 8 shows schematically the coordinates currently used for analysis of DS of a lamellar eutectic, where the solidifying interface was approximated by a planar case. In the present experiments, $V > 10\ \mu m\ s^{-1}$, so this approximation is valid [30]. For an abrupt change of V, the solute redistribution is needed to form a new steady-state field of diffusion from that before the abrupt change. This redistribution involved two aspects. One is an exponential-type field of diffusion in the normal direction of the solidifying interface, i.e. Z-axis. Because the diffusion length $L \simeq 10$–$100\ \mu m$, a new solute gradient along the Z-axis could be formed as the solidifying interface propagated a distance $\sim L$ after the abrupt change of V.

However, for the second aspect, the situation was totally different. The periodic distribution of solute concentration in the liquid along the solidifying interface, i.e. along the X-axis, had its wavelength equal to the spacing of the lamellar structure, although its amplitude was determined by V. As V changed suddenly, the amplitude would increase for $\rho > 1$ and decrease for $\rho < 1$. Adjustment of this wavelength can only be realized by response of the spacing. For an isotopic system, this response may be rapid. However, this response can only be finished after the solidifying interface propagated a long distance for those strong anisotropic systems, such as Al–Si eutectic, focused here. For instance, we analyse the case for $\rho > 1$. As V changed, if splitting of the silicon lamellae was very hard to achieve, the wavelength adjustment of solute distribution along the X-axis would be restrained. For the case of $\rho < 1$, a similar analysis can be made. Therefore, the response of the spacing to an abrupt change of V not only depends on the solute redistribution in a liquid, but also is controlled by splitting (for the case of $\rho > 1$) and terminating (for the case of $\rho < 1$) of the lamellar phases. This effect is termed the growth anisotropy of the lamellar phases. For Al–Si eutectic, this anisotropy effect involves two aspects: one is that the scale of the solidifying interface could not easily respond to the abrupt change of V by splitting of the two lamellar phases; other is that the termination of the lamella seemed to be very difficult dynamically in comparison with lamellar splitting. The latter was the reason why S_r for $\rho < 1$ was much larger than that for $\rho < 1$. A dynamic factor is introduced to characterize this anisotropy by solving the diffusion equation in the liquid.

4.1. Diffusion equation

In the coordinates shown in Fig. 8, the solute diffusion in the liquid after the abrupt change of V from V_1 to V_2 satisfied following time-related Laplacian equation

$$\frac{\partial^2 C}{\partial X^2} + \frac{\partial^2 C}{\partial Z^2} + \frac{V_2}{D_L}\frac{\partial C}{\partial Z} = \frac{\partial C}{D_L \partial t} \tag{2}$$

where C is the solute concentration in the liquid and t is the time. In this work, the structure of the Al–Si eutectic is approached by an array of lamellae, the two phases are α(Al) and β(Si), respectively. The initial and boundary conditions are

$$C = C|_{V=V_1} = C_1 \quad \text{at} \quad t = 0 \tag{3a}$$

$$C = C_E \quad \text{as} \quad Z \to \infty \tag{3b}$$

$$\frac{\partial C}{\partial X} = 0 \quad \text{as} \quad X = 0 \quad \text{and} \quad S_\alpha + S_\beta \tag{3c}$$

where C_E is the concentration at the eutectic point, C_1 is the solute distribution in the liquid as the solidifying interface propagates at a constant rate, V_1, which can be written following the approach of Jackson and Hunt [11]

$$C_1 = C_E + \sum_{n=1}^{\infty} \frac{\lambda_1 V_1 C_0}{(n\pi)^2 D_L} \sin\left(\frac{n\pi}{1+\varepsilon}\right) \cos\left(\frac{2n\pi X}{\lambda}\right) \times \exp(-M_1 Z) \tag{4}$$

where $\lambda_1 = \lambda_{S1}$, C_0 is the gap between the maximum solubilities of α and β phases, $\varepsilon = S_\beta/S_\alpha$, M_1 has the following expression

$$M_1 = \frac{V_1}{2D_L} + \left[\left(\frac{V_1}{2D_L}\right)^2 + \left(\frac{2n\pi}{\lambda_1}\right)^2\right]^{1/2} \tag{4a}$$

Suppose Equation 2 has a solution of the form

$$C = A(X)B(Y)Y(t) \tag{5}$$

substituting Equation 5 into Equation 2, we obtain

$$\frac{1}{D_L Y(t)}\frac{dY(t)}{dt} = \gamma_1 \tag{6a}$$

$$\frac{1}{A(X)}\frac{d^2 A(X)}{dX^2} = -\gamma_2 \quad \text{where } \gamma_2 > 0 \tag{6b}$$

$$\frac{1}{B(Z)}\frac{d^2B(Z)}{dZ^2}+\frac{V_1}{D_L B(Z)}\frac{dB(Z)}{dZ} = \gamma_3$$

where $\gamma_3 > 0$ (6c)

$$\gamma_1 + \gamma_2 = \gamma_3 \quad (6d)$$

It is obvious that both γ_1 and γ_2, and then γ_3, should be constant because Equation 6a, b and c are non-correlating.

Equation 6a–c can be solved. Substituting these solutions into Equation 5 and then a summation of Equation 5 over $n = 1$ to $n \to \infty$ creates a Fourier series expression of the variable C

$$C = \sum_{n=1}^{\infty} W_n \cos\left(\frac{2n\pi X}{\lambda}\right)\exp(D_L\gamma_1 t - M_2 Z) \quad (7a)$$

where W_n is an integral constant to be determined and M_2 is

$$M_2 = \frac{V_2}{2D_L} + \left[\left(\frac{V_2}{2D_L}\right)^2 + \gamma_3\right]^{1/2} \quad (7b)$$

From Equation 3b, we easily get $C = C_E$ as a solution of Equation 2, so we have

$$C = C_E + \sum_{n=1}^{\infty} W_n \cos\left(\frac{2n\pi X}{\lambda}\right)\exp(D_L\gamma_1 t - M_2 Z) \quad (8)$$

Evaluation of constant W_n depends on the response of λ to abrupt change of V. As observed experimentally, this response was gradual and smooth with time. Therefore, the period of C along the X-axis must change gradually but not suddenly as the response to an abrupt change of V. By this approach, we have another initial condition

$$M_1 = M_2, \quad \lambda = \lambda_1 = \lambda_{S1} \quad \text{at} \quad t = 0 \quad (9)$$

Comparing Equations 4 and 8 by setting $t = 0$, we derive the expression of constant W_n

$$W_n = \frac{\lambda_1 V_1 C_0}{(n\pi)^2 D_L}\sin\left(\frac{n\pi}{1+\varepsilon}\right) \quad (10)$$

4.2. Growth anisotropy

The effect of growth anisotropy of two lamellar phases has been analysed above. Because the solute redistribution in a liquid became dependent on the growth anisotropy, the constant γ_1, which represents the response rate of the solute distribution with time, as defined in Equation 6a, can be introduced as a dynamic factor to characterize this effect. Because the term $|C - C_E|$ was an increasing function of time for $\rho > 1$ and a decreasing function of time for $\rho < 1$, it is easily inferred that γ_1 has the following properties

$$\gamma_1 \begin{cases} > 0 & \text{as} \quad \rho > 1 \\ = 0 & \text{as} \quad \rho = 1 \\ < 0 & \text{as} \quad \rho < 1 \end{cases} \quad (11)$$

Obviously, the smaller the term $|\gamma_1|$, the more slowly the solute field responds with time, because the stronger is the growth anisotropy of the lamellar phases. From our experiments, we can expect that the term $|\gamma_1|$ for $\rho < 1$ is smaller than that for $\rho > 1$.

4.3. Retarded distance, S_r

Having a factor to characterize the effect of the growth anisotropy, we now can formulate S_r as a function of V_1 and ρ. A quantitative comparison of the theory with the measured results becomes possible.

We denote by $\bar{C}_\alpha$ and $\bar{C}_\beta$ the average values of the solute concentration in the liquid in front of the solidifying interface of α and β lamellae respectively, which are written as

$$\bar{C}_\alpha = \frac{1}{S_\alpha}\int_0^{S_\alpha} C\,dX \quad (12a)$$

$$\bar{C}_\beta = \frac{1}{S_\beta}\int_{S_\alpha}^{S_\alpha+S_\beta} C\,dX \quad (12b)$$

We obtain

$$\bar{C}_\alpha = C_E + \lambda V_2 Q_\alpha^L \qquad 0 \le X \le S_\alpha \quad (13a)$$

$$\bar{C}_\beta = C_E - \lambda V_2 Q_\beta^L \qquad S_\alpha < X \le S_\alpha + S_\beta \quad (13b)$$

where

$$Q_\alpha^L = \frac{2(1+\varepsilon)}{D_L}\frac{\lambda_1 V_1}{\lambda V_2} C_0 P_S \exp(D_L\gamma_1 t) \quad (13c)$$

$$Q_\beta^L = \frac{2(1+\varepsilon)}{\varepsilon D_L}\frac{\lambda_1 V_1}{\lambda V_2} C_0 P_S \exp(D_L\gamma_1 t) \quad (13d)$$

$$P_S = \sum_{n=1}^{\infty}\frac{1}{(n\pi)^3}\sin^2\left(\frac{n\pi}{1+\varepsilon}\right) \quad (13e)$$

Here, as a rough approximation, the local equilibrium is assumed to be still valid. The average supercooling of the solidifying interfaces, ΔT_α and ΔT_β, can be written as

$$\Delta T_\alpha = m_\alpha(\bar{C}_\alpha - C_E) + a_\alpha/\lambda \qquad m_\alpha > 0, \quad 0 \le X \le S_\alpha \quad (14a)$$

$$\Delta T_\beta = -m_\beta(\bar{C}_\beta - C_E) + a_\beta/\lambda \qquad m_\beta > 0, \quad S_\alpha < X \le S_\alpha + S_\beta \quad (14b)$$

where m_α and m_β are the absolute liquidus slopes of α and β phases, a_α and a_β are the Gibbs–Thonson coefficients of α/L and β/L interfaces defined by Jackson and Hunt [11], respectively. Under DS conditions, the two lamellar phases have the same supercooling, ΔT, on the solidifying interface, so we obtain

$$\Delta T = \Delta T_\alpha = \Delta T_\beta = (\Delta T_\alpha + \Delta T_\beta)/2 = m(Q^L\lambda V_2 + a^L/\lambda) \quad (15)$$

where

$$m = m_\alpha m_\beta/(m_\alpha + m_\beta)$$

$$Q^L = \frac{(1+\varepsilon)^2}{\varepsilon D_L}\frac{\lambda_1 V_1}{\lambda V_1} C_0 P_S \exp(D_L\gamma_1 t)$$

$$a^L = (a_\alpha + a_\beta)/2m$$

Following the extremum condition proposed by Jackson and Hunt [11], we have the scaling law

$$\lambda^2 V_2 = a^L/Q^L \quad (16a)$$

For DS of Al–Si eutectic, with $V > 10\ \mu m\,s^{-1}$, this scaling law is still valid if a factor k is added [28]

$$\lambda^2 V_2 = ka^L/Q^L \quad (16b)$$

On the other hand, we have

$$\lambda_{S1}^2 V_1 = ka^L \Big/ \left(\frac{(1+\varepsilon)^2}{\varepsilon D_L} C_0 P_S\right) = W_S(\text{const.}) \quad (17a)$$

$$\lambda_{S2}^2 V_2 = ka^L \Big/ \left(\frac{(1+\varepsilon)^2}{\varepsilon D_L} C_0 P_S\right) = W_S(\text{const.}) \quad (17b)$$

where W_S can be obtained from our measurements [27]. Combining Equations 16b and 17, we obtain the time, t_r, needed for λ shifting from λ_{S1} to λ_{S2} as

$$t_r = \frac{V_1/V_2}{2D_L\gamma_1}\rho \ln \rho \quad (18a)$$

hence the retarded distance $S_r = t_r V_2$ is

$$S_r = \frac{V_1}{2D_L\gamma_1}\rho \ln \rho \quad (18b)$$

4.4. Comparison with experiments

For Al–Si eutectic, $D_L = 5000\ \mu m^2\,s^{-1}$ [30]. By taking $\gamma_1 = 3.0 \times 10^{-3}/D_L\,s^{-1}$ for $\rho > 1$ and $V_1 = 10\ \mu m\,s^{-1}$, and $\gamma_1 = -6.0 \times 10^{-4}/D_L\,s^{-1}$ for $\rho < 1$ and $V_1 = 100\ \mu m\,s^{-1}$, the calculated S_r as a function of ρ has been presented in Figs 4 and 6. The excellent agreement of the calculated S_r with the measured S_r is clearly shown. When $\rho < 1$, there exists a maximum value of S_r, denoted by $(S_r)_{max}$, at $\rho = 1/e \cong 0.37$. This is also roughly consistent with the measured results, as shown in Fig. 6.

Applying Equation 18b to these cases shown in Fig. 3, we have:

$a \Rightarrow b$: $V_1 = 6.89\ \mu m\,s^{-1}$, $\rho = 3.35$,
$S_{rc} = 5.11$ mm, $S_{rm} = 5.0$ mm

$b \Rightarrow c$: $V_1 = 24.33\ \mu m\,s^{-1}$, $\rho = 2.17$,
$S_{rc} = 6.85$ mm, $S_{rm} = 7.0$ mm

$c \Rightarrow d$: $V_1 = 52.91\ \mu m\,s^{-1}$, $\rho = 1.72$,
$S_{rc} = 8.25$ mm, $S_{rm} = 9.5$ mm

where S_{rc} is the calculated S_r and S_{rm} is the measured S_r.

Similarly, applying it to the cases shown in Fig. 5, we obtain:

Fig. 5a: $V_1 = 66.97\ \mu m\,s^{-1}$, $\rho = 0.67$,
$S_{rc} = 14.93$ mm, $S_{rm} = 14.00$ mm
$V_1 = 46.95\ \mu m\,s^{-1}$, $\rho = 0.48$,
$S_{rc} = 13.79$ mm, $S_{rm} = 11.00$ mm

Fig. 5b: $V_1 = 68.65\ \mu m\,s^{-1}$, $\rho = 0.14$,
$S_{rc} = 15.94$ mm, $S_{rm} = 20.00$ mm

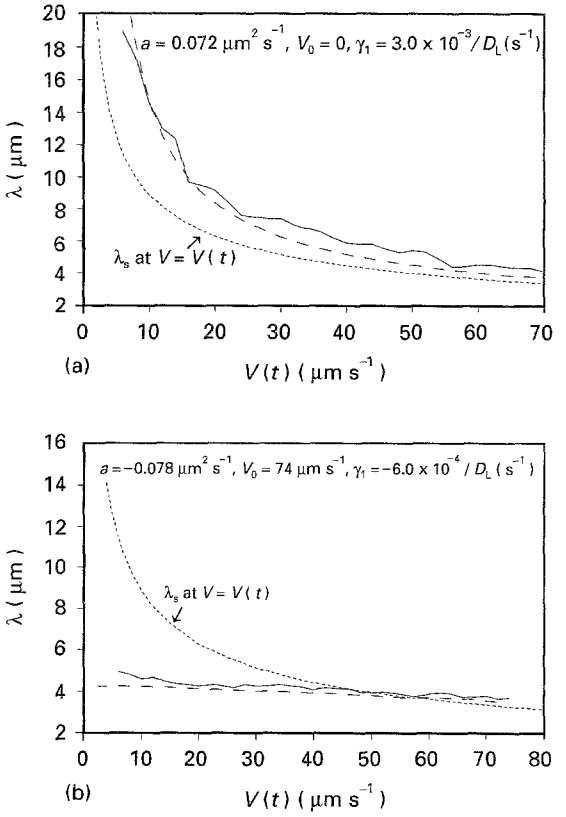

Figure 9 The (– – –) calculated and (——) measured response curves of the spacing λ to (a) constant accelerating solidification rate and (b) to constant decelerating solidification rate. Here the response is represented by plotting the spacing against the solidification rate.

Good consistency between S_{rc} and S_{rm} has also been revealed.

As presented above, for Al–Si eutectic, we should have $|\gamma_1|_{\rho>1} > |\gamma_1|_{\rho<1}$. This inequality is supported by our theoretical approach. Therefore, we can conclude that the present theory is a valid approach to the response dynamics of the lamellar spacing to an abrupt change of V.

4.5. Application to other cases

Although the theoretical approach presented above was derived for the response of λ to an abrupt change of V, it can also be applied to other non-steady-state cases. In any case, V can be formulated as a function of time, $V(t)$. In addition to the case with abrupt change of V, ρ as a function of time can then be expressed as

$$\rho(t) = V(t + dt)/V(t) \quad (19)$$

In a previous report [26] we studied the response of spacing λ to a constant accelerating solidifying interface for DS of Al–Si eutectic, with an acceleration a satisfying $|a| \ll 1.0\ \mu m^2\,s^{-1}$. The solidifying rate, $V(t)$, at time t is

$$V(t) = V_0 + at \quad (20)$$

with V_0 being the initial rate. From Equation 18b, we have

$$S_r = \frac{V_0 + at}{2D_L\gamma_1}\rho(t)[\rho(t) - 1] \quad (21)$$

Substituting Equations 19 and 20 into Equation 21, we obtain

$$S_r = \int_0^t \frac{a\,dt}{2D_L\gamma_1} = \frac{V(t) - V_0}{2D_L\gamma_1} \quad (22)$$

Considering Equation 17 and the relation $V(t_2)^2 = V(t_1)^2 + 2aS_r$, we obtain the response of λ as a function of $V(t)$:

$$\lambda^2 = W_1/[V(t)^2 - 2aS_r]^{1/2} \quad (23)$$

with $[V(t)^2 - 2aS_r] > 0$.

Fig. 9a and b show the calculated and measured response curves with $a > 0$ and $a < 0$, respectively, where the spacing, λ, was plotted against $V(t)$. The excellent agreement between them shows that the present approach is also valid for describing the response dynamics of the spacing, λ, during other non-steady-state DS of a lamellar eutectic. This fact again reveals that the constant γ_1, as defined by Equation 6a, is an effective dynamic factor to characterize the growth anisotropy effect of the eutectic phases. For Al–Si eutectic, $\gamma_1 = 3.0 \times 10^{-3}/D_L\ s^{-1}$ as propagation of the solidifying interface is being accelerated, and $\gamma_1 = -6.0 \times 10^{-4}/D_L\ s^{-1}$ as the interface is being decelerated.

5. Conclusion

The response dynamics of the lamellar spacing, λ, to an abrupt change of the solidifying rate, V, for Al–Si eutectic during DS has been investigated experimentally. The measurements have shown that the response was gradual and seriously retarded, with the retarded distance, S_r, as a function of the abrupt change factor, ρ, and the solidifying rate, V_1, before the abrupt change. The structure response mechanisms were "cluster branching" for $\rho > 1$ and "cluster terminating" plus "cluster branching" for $\rho < 1$, of the lamellar phases. The uniqueness of the spacing selection has been verified experimentally. A theoretical approach to the response dynamics has been developed by considering the response of the solute diffusion in the liquid to the abrupt change of V, and the effect of growth anisotropy of the lamellar phases. A dynamic factor, γ_1 to characterize the effect of growth anisotropy has been introduced. For $\rho > 1$, $\gamma_1 = 3.0 \times 10^{-3}/D_L\ s^{-1}$, and $\gamma_1 = -6.0 \times 10^{-4}/D_L\ s^{-1}$ for $\rho < 1$. An analytical expression of the retarded distance, S_r has been derived

$$S_r = \frac{V_1}{2D_L\gamma_1}\rho \ln\rho$$

The present approach shows excellent agreement with the measured results, and has been successfully applied to describe the non-steady-state DS with constant accelerating (decelerating) solidification rate.

Acknowledgements

The authors thank Ms P. Zhang and Mr F. Zhang for their help in the preparation of the manuscript. The financial support from the National Natural Science Foundation of China is acknowledged.

References

1. D. M. STEFANESCU, G. J. ABBASCHIAN and R. J. BAYUZIK (eds), "Solidification processing of eutectic alloys" (TMS, Warrendale, PA, 1988).
2. W. KURZ and P. R. SAHM, "Gerichtet erstarrte eutektische Werkstoffe" (Springer, Berlin, 1975).
3. R. ELLIOTT, "Eutectic solidification processings" (Butterworths, London, 1983).
4. H. MÜLLER-KRUMBHAAR and W. KURZ, in "Materials science and technology: a comprehensive treatment", Vol. 5, edited by R. W. Cahn, P. Haasen and E. J. Kramer (VCH, New York, 1991) p. 554.
5. J. S. LANGER, *Phys. Rev. Lett.* **44** (1980) 1023.
6. V. DATYE and J. S. LANGER, *Phys. Rev. B* **24** (1981) 4155.
7. B. CAROLI, C. CAROLI and B. ROULET, *J. Phys. (Fr)* **51** (1990) 1865.
8. A. KARMA, *Phys. Rev. Lett.* **59** (1987) 71.
9. V. SEETHARAMAN and R. TRIVEDI, *Metall. Trans. A* **19** (1988) 2955.
10. D. KESSLER, J. KOPLIK and H. LEVINE, *Adv. Phys.* **37** (1988) 255.
11. K. A. JACKSON and J. D. HUNT, *Trans. Metall. AIME* **236** (1966) 1129.
12. T. SATO and Y. SAYAMA, *J. Crystal Growth* **22** (1974) 529.
13. G. E. NASH, *ibid.* **38** (1977) 55.
14. D. J. FISHER and W. KURZ, *Acta. Metall.* **28** (1980) 777.
15. K. PANDLEY and P. RAMACHANDRARAO, *ibid.* **35** (1987) 2549.
16. J. M. LIU, Z. G. LIU and Z. C. WU, *Mater. Sci. Eng. A.* **167** (1993) 87.
17. K. KASSNER and C. MISBAH, *Phys. Rev. Lett.* **65** (1990) 1458.
18. *Idem, ibid.* **66** (1991) 445.
19. *Idem, Phys. Rev. A* **44** (1991) 6513.
20. *Idem, ibid.* **44** (1991) 6533.
21. K. KASSNER, A. VALANCE, C. MISBAH and D. TEMKIN, *Phys. Rev. E* **48** (1993) 1091.
22. M. R. MOLLARD and M. C. FLEMINGS, *Trans. Metall. AIME* **239** (1967) 1526.
23. *Idem, ibid.* **239** (1967) 1534.
24. T. CARLBERG and H. FREDRIKSSON, *J. Crystal Growth* **42** (1977) 526.
25. L. CLAPHAM and R. W. SMITH, *ibid.* **79** (1986) 866.
26. J. M. LIU, Y. H. ZHOU and B. L. SHANG, *Acta. Metall. Sin. B* **3** (1990) 166.
27. *Idem, J. Mater. Sci.* **27** (1992) 2067.
28. *Idem, Acta. Metall.* **38** (1990) 1632.
29. J. M. LIU, *Mater. Lett.* **10** (1991) 521.
30. J. M. LIU, Z. G. LIU and Z. C. WU, *J. Mater. Sci.* **29** (1994) 3085.

Received 19 April 1994
and accepted 7 June 1995